

Article

## Methodologies and Uncertainties in the Use of the Terrestrial Chlorophyll Index for the Sentinel-3 Mission

Francesco Vuolo <sup>1,\*</sup>, Jadunandan Dash <sup>2</sup>, Paul J. Curran <sup>3</sup>, Dulce Lajas <sup>4</sup> and Ewa Kwiatkowska <sup>5</sup>

<sup>1</sup> Institute of Surveying, Remote Sensing and Land Information (IVFL), University of Natural Resources and Life Sciences (BOKU), Peter Jordan Str. 82, A-1190 Vienna, Austria

<sup>2</sup> School of Geography, University of Southampton, Highfield, Southampton SO17 1BJ, UK; E-Mail: j.dash@soton.ac.uk

<sup>3</sup> City University London, Northampton Square, London EC1V 0HB, UK; E-Mail: Paul.Curran@city.ac.uk

<sup>4</sup> European Space Research and Technology Centre (ESTEC), European Space Agency (ESA), Keplerlaan 1, P.O. Box 299, 2200 AG Noordwijk, The Netherlands; E-Mail: Dulce.Lajas@esa.int

<sup>5</sup> EUMETSAT, Eumetsat Allee 1, D-64295 Darmstadt, Germany; E-Mail: Ewa.Kwiatkowska@eumetsat.int

\* Author to whom correspondence should be addressed; E-Mail: francesco.vuolo@boku.ac.at; Tel.: +43-1-47654-5135.

Received: 15 March 2012; in revised form: 12 April 2012 / Accepted: 13 April 2012 /

Published: 25 April 2012

---

**Abstract:** A methodology is described for the validation of Medium Resolution Imaging Spectrometer (MERIS) Terrestrial Chlorophyll Index (MTCI) data over heterogeneous land surfaces in an agricultural region in Southern Italy. The approach involves the use inverse canopy reflectance modeling techniques to derive maps of canopy chlorophyll content (CCC) and leaf area index (LAI) at fine spatial resolution. Indirect field measurements are used for validation of the fine spatial resolution data. Subsequently, these maps are aggregated based on a regular grid at 1 km spatial resolution to validate MERIS Level 2 MTCI (300 m). RapidEye satellite sensor data with a pixel size of 6.5 m are used for this purpose. Based on a set of independent ground measurements, fine spatial resolution maps achieved an  $R^2 = 0.78$  and  $RMSE = 0.39$  for CCC and  $R^2 = 0.76$  and  $RMSE = 0.64$  for LAI. The relationship between MERIS L2 MTCI and CCC [ $\text{g}\cdot\text{m}^{-2}$ ] achieved a coefficient of determination of 0.74 and it resulted to be extremely statistically significant ( $p$ -value  $< 0.001$ ). Additionally, a relative validation of two other satellite products at medium resolution spatial scale, namely MERIS leaf area index (LAI) and

Moderate Resolution Imaging Spectrometer (MODIS) LAI was performed by comparison with the fine spatial resolution LAI map. Results indicated a better accuracy in LAI estimation of MERIS (RMSE = 0.33) compared to MODIS (RMSE = 0.81) data.

**Keywords:** Envisat-MERIS; MERIS Terrestrial Chlorophyll Index (MTCI); canopy chlorophyll content (CCC); leaf area index (LAI); Sentinel-3; OLCI Terrestrial Chlorophyll Index (OTCI)

---

## 1. Introduction

Medium spatial resolution Earth observation (EO) data are used routinely to monitor land surface characteristics from regional to global scales. Observations by NASA's Moderate Resolution Imaging Spectrometer (MODIS), CNES's Vegetation and ESA's Medium Resolution Imaging Spectrometer (MERIS) have been used to obtain systematic estimates of terrestrial biophysical variables such as Fraction of Absorbed Photosynthetically Active Radiation (fAPAR); leaf area index (LAI) [1,2]; canopy chlorophyll content (CCC) [3,4] and vegetation phenology [5]. Estimates of these variables play an important role in ecosystem modeling and broader environmental studies and contribute to our understanding of biogeochemical fluxes and global climate. For instance, fAPAR is a measure of the photosynthetic activity and so an indicator of the amount and productivity of vegetation. For example, it is used in terrestrial ecosystem models to estimate the assimilation of carbon dioxide by vegetation. LAI characterizes the leaf surface available for energy and mass exchange between surface and atmosphere. It indicates the amount of leaf material in an ecosystem, which imposes an important control on photosynthesis, respiration, rain interception and other processes that link vegetation to climate [6]. The canopy chlorophyll content is a measure of potential productivity and is a strong indicator of vegetation physiological status and health. For example, it has been used successfully for the detection of vegetation stress, photosynthetic capacity and productivity [7,8].

In the framework of the Global Monitoring for Environment and Security (GMES) initiative, algorithms to estimate land biophysical variables will be implemented in order to provide a wide range of operational services in applications such as understanding carbon and water cycle, estimating agricultural and forest productivity and monitoring environmental change. The GMES initiative will also guarantee a long-term sustainable observation ability capable of supporting the development of a family of satellites for regional, European and global scale monitoring. Within this context the European Space Agency (ESA) initiated the ocean and global land monitoring Sentinel-3 mission. This aims to provide continuity to operational services that have been developed via the European Remote Sensing (ERS) satellite and Environmental Satellite (Envisat) missions [9]. Among other sensors, the Sentinel-3 payload will include the Ocean and Land Colour Instrument (OLCI). The OLCI will be an imaging spectrometer with a spectral sampling similar to that used for sea and land monitoring in recent years by Envisat-MERIS and SPOT-Vegetation. With a spatial resolution of 300 m (for land and coastal monitoring with 1.2 km in open ocean) and an ability to sample 21 narrow spectral intervals from ultraviolet to near-infrared, OLCI is designed to provide moderate spatial resolution biophysical products operationally [9].

In the terrestrial segment of the mission, two biophysical variables will be calculated and produced as Level 2B main products: OLCI Global Vegetation Index (OGVI) and OLCI Terrestrial Chlorophyll Index (OTCI). The OGVI is related to fAPAR whereas the OTCI is related to canopy chlorophyll content (CCC). Both biophysical variables are based on the MERIS heritage of operational land products [1,3] and will provide data continuity from Envisat's launch in 2002. The OTCI will be based on the MERIS Terrestrial Chlorophyll Index (MTCI) [3], which is already routinely distributed to users at regional and global scales as standard MERIS Level 2 (L2) products or eight days composites. The MTCI exploits the shift occurring in the red edge position of the spectral reflectance of vegetation. This shift in red edge position is related to changes in CCC [10–12], and has the advantage of remaining responsive even at very high CCC where traditional vegetation indices saturate. This CCC index has been applied successfully to many applications [13–16]. The algorithm is fast, can be implemented easily with large data sets and is therefore suitable for operational purposes.

The assessment of accuracy of the data products is a pre-requisite for the provision of reliable and time-consistent datasets to monitor annual and seasonal vegetation trends. This is particularly important in the context of the GMES initiative, since the products will be used to provide value added services or will be distributed directly to users such as environmental agencies, decision and policy makers.

Sentinel-3 is scheduled for launch in 2013. However, the current available MERIS database offers an opportunity to investigate the potential of the OLCI Sentinel-3 mission and evaluate the performance of existing and new methodologies and instruments for land surface characterization.

The aim of this paper is to assess the performance of medium spatial resolution MERIS L2 MTCI products to estimate CCC. For ease of discussion we will call this 'validation'. The study also evaluates approaches to scaling biophysical variables from fine to medium spatial resolution and outlines the uncertainty associated with validation.

### *Validation of EO-Based Medium Spatial Resolution CCC Products*

The validation of CCC products derived from remotely sensed data is particularly challenging since the signal observed by satellite sensors integrates the effects of leaf biochemical components and canopy structure (*i.e.*, foliage amount, spatial arrangement and leaf orientation). Moreover, it is influenced by the intercepted radiation from other elements such as non-photosynthetic materials (branches, stems and shoots) and underlying soils [17,18]. Determination of CCC in the field requires the estimation of two variables: Leaf area index and leaf chlorophyll concentration. The product of these two variables provides an approximation of chlorophyll content at canopy level that can be compared with that observed from satellite sensors at medium spatial resolutions [19]. Several field methods have been proposed for the estimation of LAI [20] and leaf chlorophyll concentration [21,22]. Whatever procedure is adopted, each field estimate of LAI or leaf chlorophyll concentration should refer to a common elementary sampling unit (ESU) that is representative, wherever possible of one vegetation type. The spatial sampling strategy (e.g., transects, grid sampling, random, *etc.*) and intensity (number of measurements per ESU) can vary depending on the equipment, canopy architecture and site homogeneity. Moreover, the extent of each ESU should correspond to the spatial resolution of remotely sensed products under validation. This is particularly complex to achieve at the

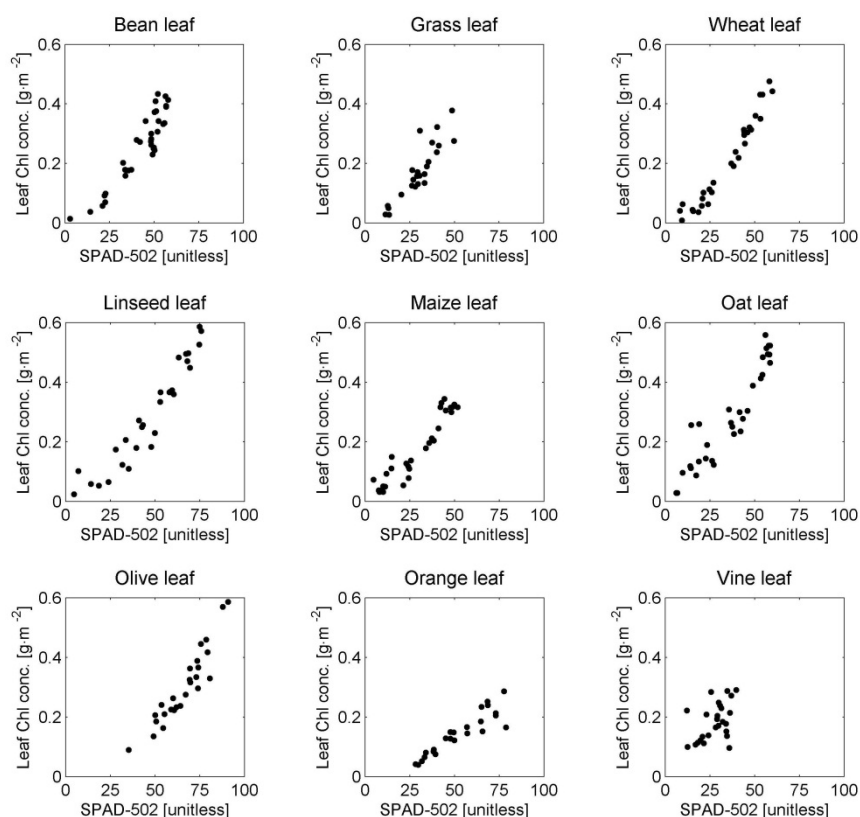
scale of medium and coarse resolution satellite sensor data due to land cover heterogeneity and poor spatial correspondence between ESU and image pixel as a result of geolocation errors [23–25]. Direct comparisons between estimates of a variable in the field and products derived from a satellite sensor data are feasible for large homogenous areas [26–28]. However, where the land surface landscape is heterogeneous, alternative validation approaches are required. Several regional and global validation studies [26,29] have used fine spatial resolution remotely sensed data (10–30 m) to map biophysical variables as an intermediate step in scale between field biophysical estimates and medium or coarser spatial resolution satellite sensor imagery. For instance, validation of MERIS biophysical variables by the VALERI group (<http://www.avignon.inra.fr/valeri/>) involved first, establishing statistical ‘transfer functions’ between fine spatial resolution (e.g., 20 m) satellite sensor images and field biophysical estimates. Then, fine spatial resolution biophysical variable maps are produced for comparison with medium spatial resolution MERIS products. This intermediate step (between field biophysical estimates to fine spatial resolution satellite sensor data) provides a more appropriate representation of spatial variability in the land surface and reduces the mismatch between field biophysical estimates (often acquired at a spatial resolution of few meters) and satellite sensor data acquired at spatial resolutions ranging from 300 m to 1 km or more. This validation approach was presented in the framework of the Land Product Validation Subgroup of the Committee on Earth Observation Satellites (CEOS) [29] as the ‘bottom-up’ approach to validation of LAI products at a global scale from field biophysical measurements.

Indirect (and typically non-destructive) measurement techniques have been used to estimate LAI and leaf chlorophyll concentration in the field because they are simple and time efficient when compared to direct (and typically destructive) measurement techniques. Indirect measurement techniques when used adequately can provide estimates that are close to direct measurements for a range of vegetation types and conditions and can be used speedily over large areas [30]. For instance, LAI estimates can be derived using the Li-Cor LAI-2000 sensor (Li-Cor, Inc. USA); digital hemispherical photography (DHP) [20]; quantum sensors, such as TRAC (3<sup>rd</sup> Wave Engineering, ON, Canada) and Decagon AccuPAR (Decagon Devices, Inc.) or ceptometers (Delta-T devices Ltd, UK). However, hemispherical sensors (such as LAI-2000 and DHP) have been shown to be more robust than other sensors [31,32] in terms of their limited sensitivity to environmental conditions, operational procedures and assumptions, for example in relation to canopy architecture. The LAI-2000 instrument uses a fish-eye lens to measure the canopy light interception in multiple directions at five angles. LAI and the foliage mean tilt angle (MTA) are then estimated directly by inverting a simple radiative transfer model for vegetative canopies [33]. The digital hemispherical photography technique is based on upward-looking fish-eye photographs taken from beneath the plant canopy that are processed using dedicated software to estimate LAI [34,35]. A detailed review of field techniques for the estimation of LAI can be found in [20,30–32].

Non-destructive estimates of leaf chlorophyll concentration can be obtained from portable leaf chlorophyll meters such as a Minolta SPAD-502 (Minolta Camera Co. Ltd., Japan) or an Opti-Sciences CCM-200 meter (Opti-Sciences, Inc., USA). These instruments use transmitted radiation in selected visible wavelengths to estimate chlorophyll concentration in leaves. Although such contact devices are quicker than destructive sampling, the measurements of transmission represent relative values of chlorophyll concentration and are very sensitive to leaf structural properties such as thickness, density,

cuticle thickness and pubescence [36–38]. However quantitative leaf chlorophyll concentration estimates can be obtained using a conversion equation derived from destructive extraction procedures [21] and contemporaneous contact non-destructive measurements. While a useful approach, [39–41] have reported curvilinear relationship with sensor sensitivity declining at higher levels of leaf chlorophyll concentration [42–46]. An overview of the scatter around relationships between SPAD-502 readings and leaf chlorophyll concentration is presented in Figure 1. Based on this dataset acquired in our past experimental campaigns linear relationships are observed for the majority of leaf types.

**Figure 1.** An overview of the scatter around relationships between SPAD-502 readings and leaf chlorophyll concentration extracted in the laboratory for nine leaf types. This dataset is part of our past experimental campaigns and destructive chlorophyll extraction was performed according to the procedures described in [47,48].



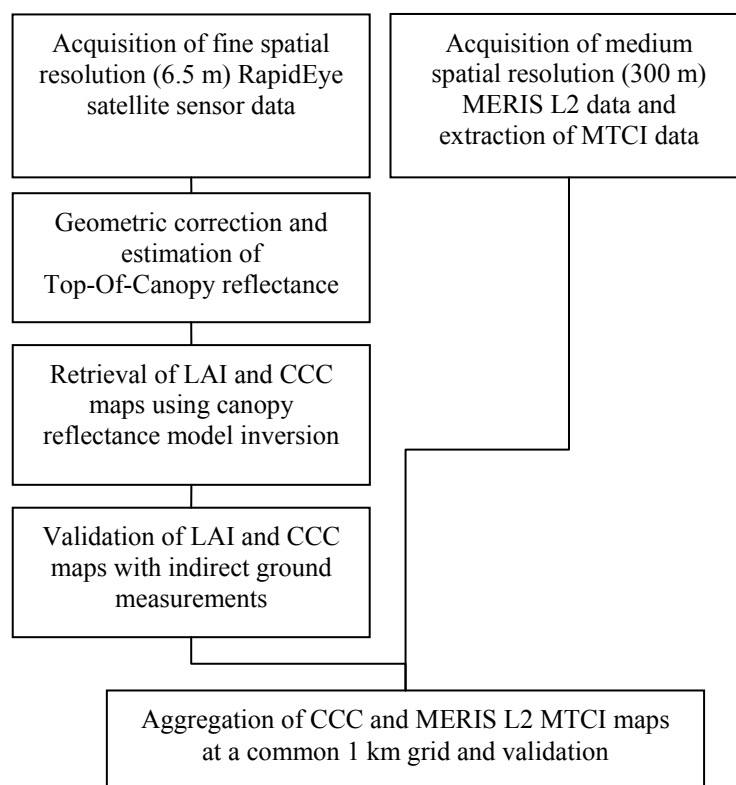
## 2. Experimental Data

### 2.1. Overview

In this study, high spatial resolution maps of LAI and CCC were derived using inverse canopy reflectance modeling with RapidEye imagery. The resulting maps were aggregated at 1 km spatial resolution to validate MERIS L2 MTCI. Field measurement techniques were used during an experimental campaign to estimate LAI and leaf chlorophyll concentration and to validate fine spatial resolution LAI and CCC maps. Generalized and, where possible, canopy specific conversion equations were used to estimate leaf chlorophyll concentration from SPAD-502 measurements. A schematization of the validation processing is presented in Figure 2. Particular attention was dedicated to LAI; a

relative validation of two other satellite products at medium resolution spatial scale, namely MERIS LAI and MODIS LAI, was performed by comparison with the fine spatial resolution LAI map.

**Figure 2.** Schematization of the validation process for the Medium Resolution Imaging Spectrometer (MERIS) L2 Terrestrial Chlorophyll Index (MTCI) data. Similarly, this validation scheme was used for MERIS and Moderate Resolution Imaging Spectrometer (MODIS) leaf area index (LAI) data.



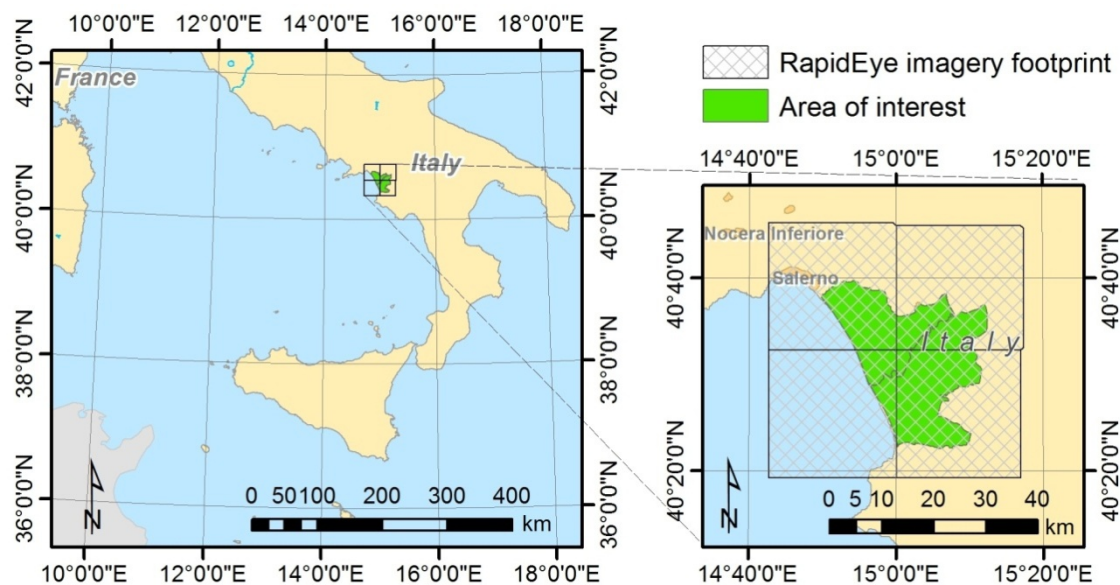
## 2.2. Field Campaign

This study was undertaken at the 560 km<sup>2</sup> ‘Piana del Sele’ site in the Campania region of Southern Italy (Figure 3) (Lat. 40.52°N, Long. 15.00°E). The study site, one of the largest agricultural areas in the region, is characterized by irrigated agriculture (mainly forage crops, fruit trees and vegetables) with an average field size of about 2 ha [47]. Within this large and relatively flat region, LAI and leaf chlorophyll concentration were estimated within 400 m<sup>2</sup> elementary sampling units (ESU) that were relatively homogeneous in terms of both vegetation type and growth stage. The center of each ESU was geo-located by means of a GPS, with an accuracy of ±3–5 m.

LAI and leaf chlorophyll concentration were estimated using a random sampling scheme within each of 36 ESUs. These ESUs were located in the study site according to field accessibility but were distributed within the area of interest to cover a variety of crop conditions. A LAI map derived from a SPOT fine spatial resolution image acquired on 12 August 2009 was used to locate possible fields for LAI and CCC sampling. The SPOT-LAI map was derived using a semi-empirical relationship based on the Weighted Difference Vegetation Index (WDVI). A logarithmic relationship was used to estimate LAI from WDVI, which was calibrated during several field campaigns in the study site in the

last years ( $R^2 = 0.64$ ) [48]. LAI and leaf chlorophyll concentration were sampled within ESUs over a period of three days (from 23 to 25 August 2009) for a range of crops including forage crops (1 alfalfa and 11 maize ESUs), fruit trees (1 plum, 2 apricot, 5 kiwi and 11 peach ESUs) and vegetables (1 aubergine, 1 pepper, 1 artichoke ESU). In addition two high-biomass poplar plots were also sampled.

**Figure 3.** The study was carried out in Campania region in Southern Italy (**left**). The test site was located in the ‘Piana del Sele’ (**right**), one of the largest agricultural areas in the region. The gridded box represents the footprint of the 4 RapidEye image tiles used in the study.



LAI was estimated using the Plant Canopy Analyser LAI-2000. The instrument has four well-documented limitations and two of these were dealt with explicitly in this study. Measurements were made during early morning and late afternoon under diffuse light conditions to minimize the effects of direct sunlight and thereby minimize LAI underestimation [49]. A view cap of 180 degrees was used to physically limit the sensor field-of-view and thus to reduce interference due to the presence of an operator. However, it was accepted that the sensor did not distinguish photosynthetically active leaf tissue from other plant elements, such as stems, flowers or senescent leaves and so LAI would be overestimated, especially in woody species. By contrast, the ‘clumping effect’, *i.e.*, non-random positioning of canopy elements, was also neglected causing LAI underestimation. Different definitions of LAI have been used in the literature depending on vegetation type and measurement device [31]. These have included green LAI [50], effective LAI [51] and plant area index [52]. The ‘LAI’ recorded using the LAI-2000 sensor represents a measure close to the effective Plant Area Index (‘PAIe’) [53,54] for reasons discussed above. The average LAI, resulting from two replications of one above-canopy and nine below-canopy measurements, was taken as representative measure for each ESU. The two replications (for a total of 18 measurements) were sampled randomly within the ESU. LAI values within the 36 ESUs ranged between 0.5 and 5.5 with a mean of 2.2 and a standard deviation of 1.3.

Leaf chlorophyll concentration was estimated using the SPAD-502 chlorophyll meter. At each ESU, 30 random measurements of leaves in different canopy layers were averaged to produce one value. Destructive sampling was not possible during the campaign. Therefore crop-specific conversion

equations were taken from the literature (peach, apricot, plum trees: [55]; maize: [56]; and a generalized conversion equation for the other vegetation types: [57]) and used to convert SPAD-502 values to leaf chlorophyll concentration [ $\text{g}\cdot\text{m}^{-2}$ ] (see Table 1).

**Table 1.** Conversion equations used to convert relative SPAD-502 values to leaf chlorophyll concentration.

Vegetation Type	Conversion Equation	$R^2$
Fruit trees <sup>(1)</sup>	$y = 0.0102 x - 0.079$	0.83
Maize <sup>(2)</sup>	$y = 0.0109 x - 0.097$	0.80
Other types above <sup>(3)</sup>	$y = 0.00859 x$	0.69

Conversion equations [ $\text{g}\cdot\text{m}^{-2}$ ] according to: <sup>(1)</sup> [55], <sup>(2)</sup> [56], <sup>(3)</sup> [57].

SPAD-502 values within the 36 ESUs ranged between 30 and 68 with a mean of 48 and a standard deviation of 10. The total CCC for an indicative  $\text{m}^2$  of ground was obtained by multiplying leaf chlorophyll content with the corresponding LAI of each ESU. The mean and standard deviation for LAI and CCC field estimates are provided in Table 2. Though care was taken to distribute the ESUs within the study site, their locations were restricted to fields with good access, which could have introduced a bias in the field data collection.

**Table 2.** Mean values (and standard deviation) of LAI and CCC field estimates.

Vegetation Type	LAI [unitless]	CCC [ $\text{g}\cdot\text{m}^{-2}$ ]
Fruit trees	1.56 (0.49)	0.69 (0.29)
Maize	3.72 (0.89)	2.16 (0.58)
Other types above	2.09 (2.03)	1.0 (0.74)

### 2.3. Fine Spatial Resolution Data from RapidEye Constellation

Multispectral data were acquired on 17 August 2009 (at 10:35 UTC) from Choros, a satellite in the RapidEye constellation. The sensor records radiance in five broad spectral bands corresponding to blue, green, red, red-edge and near-infrared part of the electromagnetic spectrum at a spatial resolution of 6.5 m. Four scenes, acquired within a few seconds, with a maximum across-track incident angle of  $5^\circ$  were adequate to cover the study site (about  $560 \text{ km}^2$ ). Radiometrically calibrated Level 3A data were provided with a geometric accuracy of 13.95 m (root-mean-square-error, RMSE = 6.50 m). Further geometric correction was performed using Ground Control Points (GCPs) and the scenes were resampled using the nearest neighbor method, resulting in a final geo-location accuracy of about 3 m, which is consistent with the area of the ESU ( $20 \times 20 \text{ m}$ ) and allows a small cluster of pixels to be averaged and compared with field estimates. One scene, containing identifiable ground targets (*i.e.*, asphalt, sea water, concrete and sand), was atmospherically corrected by using ATCOR-2 [58]. The known spectral reflectance of these targets was used for the parameterization of the atmospheric radiative transfer model. Subsequently, an empirical line method was applied to normalize the other three scenes to the first image. For this purpose, uniform areas in the overlapping regions between

adjacent images were considered: Twenty zones of about 200 m<sup>2</sup> representing dark and bright surfaces were selected for each image and correction functions were derived for each spectral band.

#### 2.4. Medium Spatial Resolution Data from MERIS

The MERIS L2 image used in this study was acquired on 17 August 2009 (at 10:33 UTC) at a spatial resolution of approximately 300 m (full resolution) and made available through the ESA EO-LISA archive. The MERIS L2 data are accompanied by different types of geophysical information (according to the level of geophysical processing for ‘Land’, ‘Water’ and ‘Cloud’), Rayleigh-corrected reflectances and bottom-of-atmosphere vegetation indices, such as MTCI. The image geometric correction was performed using the map projection tool (nearest neighbor resampling method) implemented in the Basic ENVISAT Toolbox for (A)ATSR and MERIS (BEAM).

The MERIS top-of-canopy (TOC) vegetation algorithm (implemented as a plug-in ‘TOC-VEG’ in the ESA BEAM VISAT software) was used to estimate LAI from MERIS L2 reflectance data. As detailed in the algorithm description, TOC-VEG [27,59] is a model-inversion technique applied to a coupled leaf (PROSPECT, [60]) and canopy (SAIL, [61]) model. By means of a neural network four vegetation biophysical variables are derived: fAPAR, fCover, LAI and LAI×chlorophyll content.

#### 2.5. Medium Spatial Resolution Data from MODIS

The MODIS LAI product (tile h19v04) was collection 5 (MOD15A2), 8-day composite (from 13 to 20 August 2009), atmospherically-corrected, and at a 1 km spatial resolution. Data were made available through the Earth Resources Observation System (EROS) Data Centre Distributed Active Archive Center. The MODIS LAI product was derived using a Look-Up-Table (LUT), called the ‘main algorithm’, which provides an inversion of a three-dimensional radiative transfer (RT) model [2] within six canopy biomes: Grasses and cereal crops, shrubs, broadleaf crops, savannah, broadleaf and needle-leaf forests [62]. However, the main LAI algorithm is not applied when there are large uncertainties in surface reflectance data, misclassifications in the biome map or limitations in the LUTs [63]. Should this happen, a backup algorithm based on empirical relations between the Normalized Difference Vegetation Index (NDVI) and LAI associated with a biome classification map is triggered in order to estimate LAI. A quality flag associated to the product indicates the algorithms used for producing LAI maps. The quality flag (SFC\_QC) has five possible values; ‘0’ and ‘1’ refer to estimates by the main algorithm (LUT and RT) with ‘0’ being the ‘best’ possible result. ‘2’ and ‘3’ refer to estimates by the backup algorithm (NDVI) and ‘4’ for those that could not be estimated and so no data are given. The LAI values with the SFC\_QC = 1 are referred to saturation LAI data and they usually do not represent the LAI on the surface even though they do provide a lower limit of the ‘true’ LAI. As would be anticipated, saturation usually occurred in areas with dense canopies [64].

#### 2.6. Deriving LAI and CCC Maps from Fine Spatial Resolution Data from RapidEye Imagery

Two groups of techniques have been used to scale-up estimates of biophysical variables at the field scale in order to derive maps of those variables at fine spatial resolution [29]. The first are based on empirical equations, such as regressions between vegetation indices and field data. The second are

based on physical models (*i.e.*, inverse canopy reflectance modeling, [26]). Empirical methods are site- and sensor-specific that require accurate field data [65] and most employ vegetation indices using data in only two wavebands, usually red and near infrared [23,66]. Such simple ratios are rarely able to account for the complexity of the canopy reflected signal at fine spatial resolution as this depends also on canopy geometry (leaf inclination and spatial arrangement, plant row orientation and spacing), leaf and soil optical properties, sun position and viewing position [67,68]. A physical modeling technique was used in this study. Top-of-Canopy (atmospherically corrected) reflectance data in four wavebands (green, red, red edge, near-infrared) were used in the inversion of a leaf/canopy reflectance model to produce maps of LAI and CCC. Field data were not required for the estimation of biophysical variables and could be used exclusively for product validation, therefore avoiding circularity in the next stage of the process when an empirical relationship is derived between MTCI and CCC using chlorophyll maps derived with the same combination of wavebands.

The widely used coupled PROSPECT+SAILH model ('PROSAIL') was applied here. PROSAIL is a combination of the leaf model PROSPECT-4 [69] and the canopy model SAILH [61,70,71]. It calculates the bi-directional reflectance of homogeneous canopies as a function of several structural and biophysical variables, soil reflectance, illumination and viewing geometry. The PROSAIL model inversion was based on a LUT approach. The model was parameterized using the technique described in [72] and field measurements used to validate the accuracy of resulting LAI and CCC maps.

### *2.7. Comparing Fine Spatial Resolution CCC with Medium Spatial Resolution MERIS L2 MTCI Data*

Fine spatial resolution CCC data derived in Section 2.6 was compared with MERIS L2 MTCI. To minimize overlap errors due to pixel misalignment between the fine and the medium spatial resolution data, the fine spatial resolution map was re-projected to the same coordinate system as the medium resolution image [29]. The analysis was performed at approximately 1 km ( $3 \times 3$  full resolution MERIS pixels) spatial resolution. A regular grid was generated as an overlay to MERIS pixels. Fine spatial resolution CCC data and MERIS L2 MTCI were averaged within each grid cell.

### *2.8. Comparing Fine Spatial Resolution LAI with Medium Spatial Resolution MERIS and MODIS LAI Products*

LAI plays an important role in the validation of CCC and so an additional validation phase was used. In this step, the fine spatial resolution RapidEye satellite sensor LAI map derived in Section 2.6 was compared with the MERIS LAI and the MODIS LAI products. In the case of MERIS, the spatial aggregation was conducted as for CCC based on the 1 km grid. In the case of MODIS, a regular grid based on the position of MODIS 1 km pixels was used as the base on which to average both fine spatial resolution LAI and MODIS LAI data. The intercomparison was performed only for pixels for which there was an LAI estimate derived using the main MODIS algorithm. The selection of those pixels was achieved using the quality flag (SFC\_QC = 0) which accompanies the LAI product.

### 3. Results and Discussion

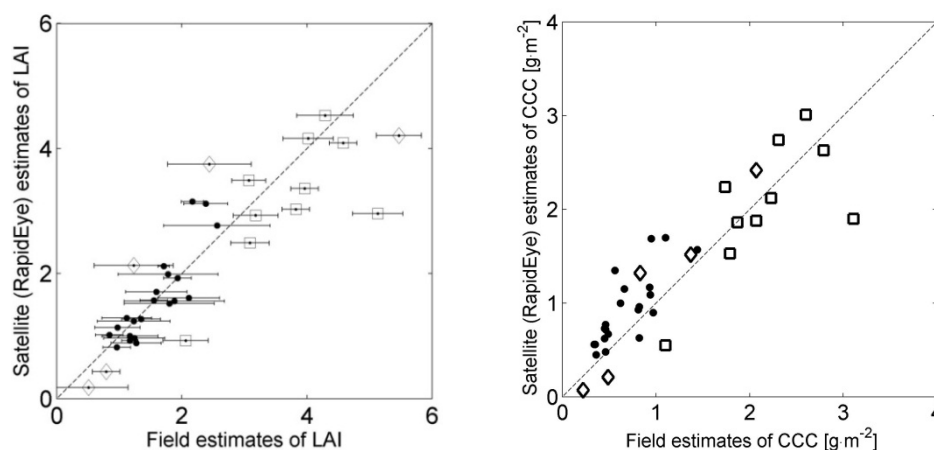
#### 3.1. Estimation of LAI and CCC from Fine Spatial Resolution Data from RapidEye Imagery: Model Inversion Results

The accuracy with which LAI and CCC can be mapped was quantified using the coefficient of determination ( $R^2$ ), the root-mean-square-error (RMSE) and the relative RMSE (RMSE/mean value of field estimates) between satellite sensor and ground based estimations. Estimations of LAI using the PROSAIL LUT model inversion approach resulted in an accuracy of  $R^2 = 0.76$ . For CCC, the estimation accuracy was  $R^2 = 0.78$ . Correlations between both LAI and CCC estimated on the ground and from satellite sensors are presented in Figure 4. The RMSE and the relative RMSE for satellite sensor estimates of LAI and CCC variables and corresponding variables estimated in the field are presented in Table 3.

**Table 3.** RMSE and relative RMSE for RapidEye satellite sensor estimates of LAI and CCC variables and corresponding variables estimated in the field.

	LAI [unitless]	CCC [ $\text{g}\cdot\text{m}^{-2}$ ]
RMSE	0.64	0.39
Relative RMSE (%)	29	34

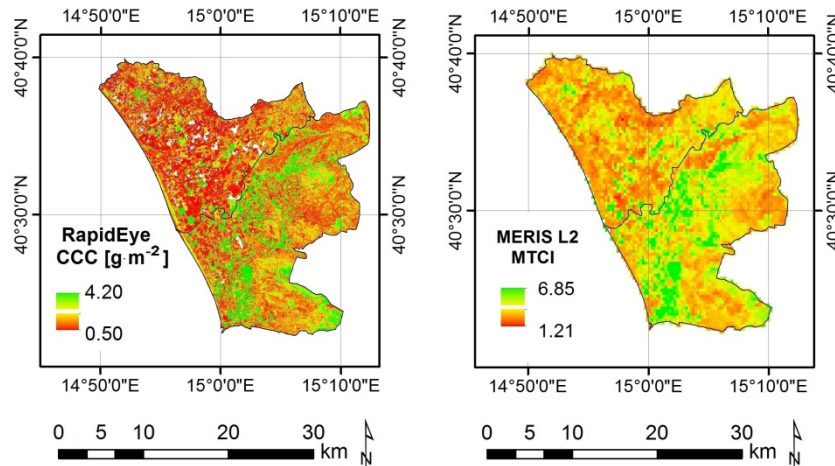
**Figure 4.** LAI (left) and CCC (right) estimated from field measurements (X axis) versus RapidEye satellite sensor data (Y axis) estimates. Symbols correspond to: ‘●’ fruit trees, ‘□’ maize and ‘◇’ other vegetation types. Error bars in LAI indicate standard deviations of the LAI estimate.



#### 3.2. Validation of Medium Spatial-Resolution MERIS L2 MTCI Data

To compare the fine and medium spatial resolution data sets, the CCC data derived from RapidEye satellite sensor data were aggregated based on a 1 km grid using the approach described in Section 2.7. Cells in which less than 80% of the area was classified as vegetation by the fine spatial resolution data were not considered further. Maps of CCC at fine spatial resolution and medium spatial resolution MERIS L2 MTCI are given in Figure 5.

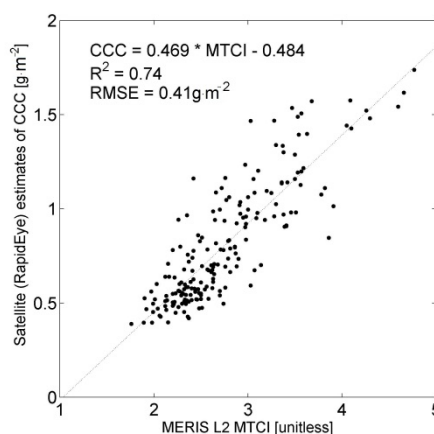
**Figure 5.** Fine spatial resolution CCC [ $\text{g}\cdot\text{m}^{-2}$ ] map from RapidEye satellite sensor data (**left**) and medium spatial resolution MERIS L2 MTCI data (**right**). The two maps were aggregated and compared at 1 km spatial resolution based on the position of MERIS pixels.



The relationship between MERIS L2 MTCI and CCC [ $\text{g}\cdot\text{m}^{-2}$ ] estimated from fine spatial resolution RapidEye satellite sensor data is presented in Figure 6. The coefficient of determination for linear equation was high ( $R^2 = 0.74$ ) and significant ( $p$ -value  $< 0.001$ ). The linear regression (no. of pixels 193) of CCC in respect to MTCI (RMSE =  $0.41 \text{ g}\cdot\text{m}^{-2}$ ) resulted in:

$$\text{CCC} [\text{g}\cdot\text{m}^{-2}] = 0.469 \text{ MTCI} - 0.484 \quad (1)$$

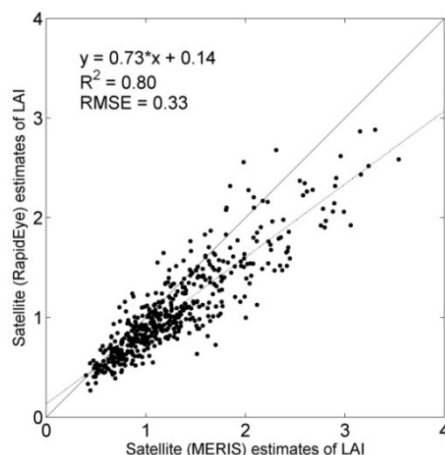
**Figure 6.** Comparison between MERIS L2 MTCI and CCC [ $\text{g}\cdot\text{m}^{-2}$ ] estimated at fine spatial resolution and aggregated at 1 km spatial resolution.



### 3.3. Comparison with Medium-Resolution MERIS and MODIS LAI Data

MERIS LAI was derived using the MERIS TOC-VEG processor implemented in BEAM VISAT software and compared to high spatial resolution RapidEye satellite sensor LAI data. The aggregation at 1 km spatial resolution was performed as described in Section 2.8. The relationship between MERIS LAI and LAI estimated from fine spatial resolution RapidEye satellite sensor data is presented in Figure 7. The coefficient of determination was high ( $R^2 = 0.80$ ) and significant ( $p$ -value  $< 0.001$ ), the RMSE resulted in 0.33 (no. of pixels 504).

**Figure 7.** Comparison between MERIS LAI (derived using the TOC-VEG processor, BEAM VISAT) and LAI estimated from RapidEye satellite sensor data aggregated at 1 km spatial resolution.



The evaluation of the MODIS LAI was performed only for those pixels flagged as best quality and processed by the main algorithm. The relationships between RapidEye satellite sensor LAI data and MODIS LAI estimated according to the MODIS three-dimensional model inversion approach is shown in Figure 8. The comparison is presented following the MODIS biome classification, which is based on six canopy architectural types (grasses and cereal crops, shrubs, broadleaf crops, savannah, broadleaf forest, and needle-leaf forest). RMSE and number of pixels for each biome type and all biomes combined are provided in Table 4.

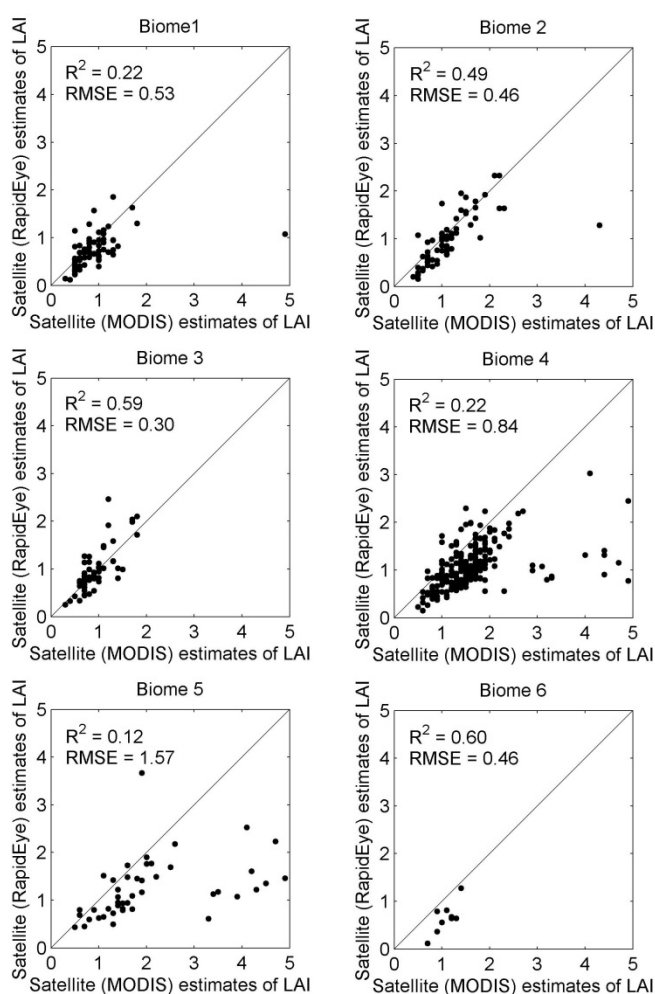
**Table 4.** RMSE and number of pixels for the relationships MODIS LAI vs. RapidEye LAI for the six biomes of the MODIS classification scheme. RapidEye LAI data were aggregated at 1 km based on the position of MODIS pixels.

Biome Code	Land Cover Type MOD12Q1	RMSE MODIS LAI – RapidEye LAI	$R^2$	No. of Pixels
1	Grasses / cereal crops	0.53	0.22	75
2	Shrubs	0.46	0.49	69
3	Broadleaf crops	0.30	0.59	57
4	Savannah	0.84	0.22	236
5	Broadleaf forest	1.57	0.12	48
6	Needle leaf forest	0.46	0.60	9
-	Combined	0.81	0.27	494

The RMSE of our validation ranged from 0.30 (broadleaf crops) to 1.57 (broadleaf forest) with a combined RMSE for the study area of 0.81. The accuracy reported for MODIS LAI (MODIS land team, <http://landval.gsfc.nasa.gov/>) is 0.66 (RMSE units). If the broadleaf forest class is excluded the resulting accuracy is 0.50. However, this accuracy is affected by (i) uncertainties in the input of the algorithm (surface reflectance and land cover) and (ii) model uncertainties, namely the consistency between RT simulations stored in the LUT and the corresponding MODIS surface reflectance [73]. Our study highlighted misclassification in the land cover product used for the LAI algorithm. For instance, 236 pixels—out of a total of 494 pixels—were classified as savannah (biome 4), whereas the

majority of the land cover is irrigated agriculture and needle leaf forest (large evergreen conifer forests are present in the coastal area of the study site). The broadleaf forest class (48 pixels), which is also rarely represented in the study area, and savannah are the two land covers with lower LAI estimation accuracy. This uncertainty is probably due to misclassification and the resultant selection of an erroneous biome type for LAI modeling.

**Figure 8.** Comparison between MODIS LAI and RapidEye LAI aggregated at 1 km spatial resolution based on the position of MODIS pixels. Results are presented according to the MODIS biome classification scheme (Biome 1: grasses and cereal crops; Biome 2: shrubs; Biome 3: broadleaf crops; Biome 4: savannah; Biome 5: broadleaf forest; Biome 6: needle leaf forest).



### 3.4. Robustness of MERIS L2 MTCI-CCC Relationships

To evaluate the robustness of MERIS L2 MTCI and CCC linear equations, different sources of uncertainty were considered. Validation of the CCC map used field estimates of LAI and leaf chlorophyll concentration, derived using indirect sampling methods. Regarding LAI field estimates, errors can be up to 10% depending on the degree of crop heterogeneity [54]. Earlier studies of LAI estimation have reported that indirect methods underestimated LAI between 25% and 30% for most woody plant canopies [74].

A major source of uncertainty in the estimation of leaf chlorophyll concentration is the definition of conversion equations used to convert field readings into leaf chlorophyll concentration. An example of the scatter around relationships between SPAD-502 readings and leaf chlorophyll concentration extracted in the laboratory is presented in Figure 1 for nine leaf types. The varying nature of the SPAD-leaf chlorophyll concentration relationships (linear and exponential) and the absence of instrument- and crop-specific conversion functions necessitate the destructive sampling of a small number of leaves in order to convert relative leaf chlorophyll concentration readings into absolute values per unit fresh weight. Using the conversion equations (not shown) derived from relationships in Figure 1 (using a minimum of 24 leaves) the best estimate of leaf chlorophyll concentration can be achieved with an error ranging from 7% to 28% (with a mean error of 12%). The robustness of the conversion equations for each of the nine crops is reported in Table 5.

**Table 5.** Coefficient of determination ( $R^2$ ), standard error and number of observations of the equations (not shown) derived from destructive sampling to convert SPAD-502 values in leaf chlorophyll concentration values. The data set is part of past experimental campaigns and destructive chlorophyll extraction was performed according to [47,48].

Crop	Wheat	Oat	Grass	Maize	Linseed	Bean	Orange	Vine	Olive
$R^2$	0.94	0.87	0.80	0.90	0.90	0.85	0.84	0.22	0.82
Standard Error [ $\text{g}\cdot\text{m}^{-2}$ ]	0.34	0.60	0.43	0.37	0.60	0.46	0.29	0.56	0.83
Observations	30	32	24	30	30	35	24	26	30

The sampling procedure is an important consideration as leaf chlorophyll concentration varies across the vertical profile of the vegetation and across different portions of the same leaf. It is recommended that the leaf surface is dry and clean (free from dust or honeydew secreted by aphids and other insects). Large variation in the measurements can be due to leaf veins and changes in thickness due to age and position of the leaf in the vertical profile. Previous studies reported that SPAD-502 readings and leaf chlorophyll concentration may also vary with plant growth stage [75], growing conditions [76], growing season [22] and genotype [77]. Thus, leaf measurement position should remain invariant within crop types. To represent the chlorophyll content in the canopy, individual leaf readings should be taken across the vertical profile of multiple plants within the same LAI sampling unit. In addition, alternative leaf chlorophyll concentration sampling strategies have been reported to increase the accuracy of CCC estimation. For instance, Gitelson *et al.* [78] estimated CCC throughout a growing season by measuring leaf chlorophyll concentration of only the upper leaves along with the LAI of the canopy. The CCC was estimated with an accuracy (RMSE) of  $0.22 \text{ g}\cdot\text{m}^{-2}$  ( $R^2 = 0.97$ ) in maize and  $0.23 \text{ g}\cdot\text{m}^{-2}$  ( $R^2 = 0.92$ ) in soybean.

An additional source of uncertainty is in the up-scaling procedures from field measurements to fine spatial resolution biophysical maps. In this study, the high-resolution CCC map was generated with a RMSE of  $0.39 \text{ g}\cdot\text{m}^{-2}$  relative to the ground measurements from 36 ESUs (Relative RMSE = 34%). This error might be due to limitations in the biophysical variable retrieval algorithm and to the ill-posed inverse problem.

Land surface heterogeneity and different plant species composition might also influence the validation results. For example, an earlier field experiment [28] provided a slightly different function compared to Equation (1) (the two equations differ with a  $p$ -value = 0.022):

$$\text{CCC} [\text{g}\cdot\text{m}^{-2}] = 0.605 \text{ MTCI} - 0.667 \quad (2)$$

In [28] field data were acquired for six vegetation species in large (>25 ha) homogenous fields. LAI and leaf chlorophyll concentration at 25 random sampling locations in each field were used to derive the chlorophyll content per field and then related to the mean MTCI value for full resolution MERIS pixels within each field.

#### 4. Conclusions

In this study, the performance of medium spatial resolution MERIS Terrestrial Chlorophyll Index Level 2 product (MERIS L2 MTCI) to estimate canopy chlorophyll content (CCC) was addressed for heterogeneous land surfaces in an agricultural region in Southern Italy.

We applied a methodology to produce a fine spatial resolution map of CCC using the inverse modeling techniques with RapidEye satellite sensor data. The validation of this map was performed with independent ground measurements. Subsequently, the CCC map (6.5 m) was aggregated to medium spatial resolution based on a regular grid (1 km) to validate MERIS L2 MTCI. A relationship between MTCI and CCC was established for land surfaces with a vegetation cover >80% at a 1 km pixel scale. Different sources of uncertainty from limitations in field measurements to scaling issues were considered and discussed. Additionally, the study concentrated on the validation of medium spatial resolution MERIS and MODIS leaf area index (LAI) products considering the same scaling approach.

In summary, results from the validation and uncertainty lead to the following conclusions:

- Medium spatial resolution MERIS L2 MTCI was validated based on fine spatial resolution CCC data derived from RapidEye satellite sensor data. The relationship between MERIS L2 MTCI and CCC [ $\text{g}\cdot\text{m}^{-2}$ ] achieved a coefficient of determination of 0.74 and it resulted extremely statistically significant ( $p$ -value < 0.001).
- Inverse modeling techniques based on a Look-Up-Table (LUT) approach were used to derive fine spatial resolution maps (6.5 m) of CCC with  $R^2 = 0.78$  and RMSE = 0.39. Similarly, LAI achieved an accuracy of  $R^2 = 0.76$  and RMSE = 0.64. The validation was based on independent LAI and leaf chlorophyll concentration estimated in 36 sampling units covering different crop species. Leaf chlorophyll concentration was estimated using the SPAD-502 chlorophyll meter.
- Based on indirect SPAD-502 measurements and crop and instrument specific conversion functions, leaf chlorophyll concentration can be estimated with an error ranging from 7% to 28% (with a mean percentage error of 12%). Wherever possible, the study suggested the use of instrument- and crop-specific conversion functions.
- The fine spatial resolution LAI map was compared to well-established medium resolution products namely MERIS LAI (based on the TOC-VEG processor implemented in the ESA BEAM VISAT software) and MODIS LAI (MOD15A2). Results indicated a better accuracy in LAI estimation of MERIS ( $R^2 = 0.80$  and RMSE = 0.33) compared to MODIS ( $R^2 = 0.27$  and

RMSE = 0.81). It was not surprising that MERIS data had a similar performance to our fine spatial resolution LAI product since both maps are based on the inversion of the same radiative transfer model. Moreover, MERIS benefits of a finer spectral and higher spatial configuration compared to MODIS. On the contrary, misclassification in the MODIS land cover biomes used for LAI modeling might be the source of uncertainty for LAI estimation.

This work provides the framework to evaluate the robustness of MERIS L2 MTCI equations and its accuracy to predict CCC. The validation protocol has been described and it will be used in future field campaigns as a standard approach to assess the performance of MTCI. Validation methodologies and quantification of uncertainties are particularly relevant in the framework of the GMES (Global Monitoring for Environment and Security) initiative, since land surface products (such as MTCI) will be distributed directly to users or will be used to provide value added services. In particular, the Sentinel-3 payload will include the Ocean and Land Colour Instrument (OLCI) and will provide the OLCI Terrestrial Chlorophyll Index (OTCI) as Level 2B main product based on the MERIS L2 MTCI heritage.

### Acknowledgments

Funding for this research was provided by ESA under the MTCI-EVAL project, additional information available at: <http://www.sen2chl.co.uk>. Logistical support for the field campaign was provided by Ariospace spin-off company (<http://www.ariespace.com>).

### References

1. Gobron, N.; Pinty, B.; Verstraete, M.; Govaerts, Y. The MERIS global vegetation index (MGVI): Description and preliminary application. *Int. J. Remote Sens.* **1999**, *20*, 1917-1927.
2. Knyazikhin, Y.; Myneni, R.B.; Tian, Y.; Wang, Y.; Zhang, Y. Estimation of Vegetation Canopy Leaf Area Index and Fraction of Photosynthetically Active Radiation Absorbed by Vegetation from Remotely Sensed Multi-Angle and Multi-Spectral Data. In *Proceedings of IEEE 1999 International Geoscience and Remote Sensing Symposium*, Hamburg, Germany, 11–13 March 1999; Volume 3, pp. 1872-1874.
3. Dash, J.; Curran, P.J. Evaluation of the MERIS terrestrial chlorophyll index (MTCI). *Adv. Space Res.* **2007**, *39*, 100-104.
4. Dash, J.; Curran, P.J. The MERIS terrestrial chlorophyll index. *Int. J. Remote Sens.* **2004**, *25*, 5403-5413.
5. Zhang, X.Y.; Friedl, M.A.; Schaaf, C.B.; Strahler, A.H.; Hodges, J.C.F.; Gao, F.; Reed, B.C.; Huete, A. Monitoring vegetation phenology using MODIS. *Remote Sens. Environ.* **2003**, *84*, 471-475.
6. Global Terrestrial Observing System (GTOS). *A Framework for Terrestrial Climate-Related Observations and the Development of Standards for the Terrestrial Essential Climate Variables: Proposed Workplan*; GTOS-77; GTOS: Rome, Italy, 2010.
7. Boegh, E.; Soegaard, H.; Broge, N.; Hasager, C.B.; Jensen, N.O.; Schelde, K.; Thomsen, A. Airborne multispectral data for quantifying leaf area index, nitrogen concentration, and photosynthetic efficiency in agriculture. *Remote Sens. Environ.* **2002**, *81*, 179-193.

8. Gitelson, A.; Vina, A.; Verma, S.; Rundquist, D.; Arkebauer, T.; Keydan, G.; Leavitt, B.; Ciganda, V.; Burba, G.; Suyker, A. Relationship between gross primary production and chlorophyll content in crops: Implications for the synoptic monitoring of vegetation productivity. *J. Geophys. Res.-Atmospheres* **2006**, *111*, 1-13.
9. Aguirre, M.; Berruti, B.; Bezy, J.-L.; Drinkwater, M.; Heliere, F.; Klein, U.; Mavrocordatos, C.; Silvestrin, P.; Greco, B.; Benveniste, J. The ocean and medium-resolution mission for GMES operational services. *ESA Bull.* **2007**, *131*, 25-30.
10. Gausman, H.W. Leaf reflectance vs. leaf chlorophyll and carotenoid concentrations for eight crops. *Agron. J.* **1977**, *69*, 799-802.
11. Dawson, T.P.; Curran, P.J. A new technique for interpolating the reflectance red-edge position. *Int. J. Remote Sens.* **1998**, *19*, 2133-2139.
12. Delegido, J.; Verrelst, J.; Alonso, L.; Moreno, J. Evaluation of Sentinel-2 red-edge bands for empirical estimation of green LAI and chlorophyll content. *Sensors* **2011**, *11*, 7063-7081.
13. Curran, P.J.; Dash, J.; Llewellyn, G.M. Indian ocean tsunami: The use of MERIS (MTCI) data to infer salt stress in coastal vegetation. *Int. J. Remote Sens.* **2007**, *28*, 729-735.
14. Wu, C.Y.; Niu, Z.; Tang, Q.; Huang, W.J.; Rivard, B.; Feng, J.L. Remote estimation of gross primary production in wheat using chlorophyll-related vegetation indices. *Agric. For. Meteorol.* **2009**, *149*, 1015-1021.
15. Zurita-Milla, R.; Kaiser, G.; Clevers, J.G.P.W.; Schneider, W.; Schaepman, M.E. Downscaling time series of MERIS full resolution data to monitor vegetation seasonal dynamics. *Remote Sens. Environ.* **2009**, *113*, 1874-1885.
16. Berberoglu, S.; Satir, O.; Atkinson, P.M. Mapping percentage tree cover from Envisat MERIS data using linear and nonlinear techniques. *Int. J. Remote Sens.* **2009**, *30*, 4747-4766.
17. Asner, G.P. Biophysical and biochemical sources of variability in canopy reflectance. *Remote Sens. Environ.* **1998**, *64*, 234-253.
18. Asner, G.P.; Wessman, C.A.; Bateson, C.A.; Privette, J.L. Impact of tissue, canopy, and landscape factors on the hyperspectral reflectance variability of arid ecosystems. *Remote Sens. Environ.* **2000**, *74*, 69-84.
19. Baret, F.; Houlès, V.; Guérif, M. Quantification of plant stress using remote sensing observations and crop models: The case of nitrogen management. *J. Exp. Bot.* **2007**, *58*, 869-880.
20. Weiss, M.; Baret, F.; Smith, G.J.; Jonckheere, I.; Coppin, P. Review of methods for in situ leaf area index (LAI) determination part ii. Estimation of LAI, errors and sampling. *Agric. For. Meteorol.* **2004**, *121*, 37-53.
21. Palta, J.P. Leaf chlorophyll content. *Remote Sens. Rev.* **1990**, *5*, 207-213.
22. Bullock, D.G.; Anderson, D.S. Evaluation of the Minolta SPAD-502 chlorophyll meter for nitrogen management in corn. *J. Plant Nutrit.* **1998**, *21*, 741-755.
23. Chen, J.M.; Pavlic, G.; Brown, L.; Cihlar, J.; Leblanc, S.G.; White, H.P.; Hall, R.J.; Peddle, D.R.; King, D.J.; Trofymow, J.A.; *et al.* Derivation and validation of Canada-wide coarse-resolution leaf area index maps using high-resolution satellite imagery and ground measurements. *Remote Sens. Environ.* **2002**, *80*, 165-184.

24. Huang, D.; Yang, W.Z.; Tan, B.; Rautiainen, M.; Zhang, P.; Hu, J.N.; Shabanov, N.V.; Linder, S.; Knyazikhin, Y.; Myneni, R.B. The importance of measurement errors for deriving accurate reference leaf area index maps for validation of moderate-resolution satellite LAI products. *IEEE Trans. Geosci. Remote Sens.* **2006**, *44*, 1866-1871.
25. Martinez, B.; Garcia-Haro, F.J.; Camacho-de Coca, F. Derivation of high-resolution leaf area index maps in support of validation activities: Application to the cropland Barrax site. *Agric. For. Meteorol.* **2009**, *149*, 130-145.
26. Tian, Y.H.; Woodcock, C.E.; Wang, Y.J.; Privette, J.L.; Shabanov, N.V.; Zhou, L.M.; Zhang, Y.; Buermann, W.; Dong, J.R.; Veikkanen, B.; *et al.* Multiscale analysis and validation of the MODIS LAI product: I. Uncertainty assessment. *Remote Sens. Environ.* **2002**, *83*, 414-430.
27. Baret, F.; Morisette, J.T.; Fernandes, R.A.; Champeaux, J.L.; Myneni, R.B.; Chen, J.; Plummer, S.; Weiss, M.; Bacour, C.; Garrigues, S.; *et al.* Evaluation of the representativeness of networks of sites for the global validation and intercomparison of land biophysical products: Proposition of the CEOS-BELMANIP. *IEEE Trans. Geosci. Remote Sens.* **2006**, *44*, 1794-1803.
28. Dash, J.; Curran, P.J.; Tallis, M.J.; Llewellyn, G.M.; Taylor, G.; Snoeij, P. Validating the MERIS Terrestrial Chlorophyll Index (MTCI) with ground chlorophyll content data at MERIS spatial resolution. *Int. J. Remote Sens.* **2010**, *31*, 5513-5532.
29. Morisette, J.T.; Baret, F.; Privette, J.L.; Myneni, R.B.; Nickeson, J.E.; Garrigues, S.; Shabanov, N.V.; Weiss, M.; Fernandes, R.A.; Leblanc, S.G.; *et al.* Validation of global moderate-resolution LAI products: A framework proposed within the CEOS land product validation subgroup. *IEEE Trans. Geosci. Remote Sens.* **2006**, *44*, 1804-1817.
30. Breda, N.J.J. Ground-based measurements of leaf area index: A review of methods, instruments and current controversies. *J. Exp. Bot.* **2003**, *54*, 2403-2417.
31. Jonckheere, I.; Fleck, S.; Nackaerts, K.; Muys, B.; Coppin, P.; Weiss, M.; Baret, F. Review of methods for in situ leaf area index determination: Part I. Theories, sensors and hemispherical photography. *Agric. For. Meteorol.* **2004**, *121*, 19-35.
32. Garrigues, S.; Shabanov, N.V.; Swanson, K.; Morisette, J.T.; Baret, F.; Myneni, R.B. Intercomparison and sensitivity analysis of leaf area index retrievals from LAI-2000, Accupar, and digital hemispherical photography over croplands. *Agric. For. Meteorol.* **2008**, *148*, 1193-1209.
33. Welles, I.J.; Norman, J.M. Instrument for indirect measurement of canopy architecture. *Agron. J.* **1991**, *83*, 818-825.
34. Rich, P.M. *A Manual for Analysis of Hemispherical Canopy Photography*; Report LA-11733-M; Los Alamos National Laboratory: Los Alamos, NM, USA, 1989.
35. Rich, P.M. Characterizing plant canopies with hemispherical photographs. *Remote Sens. Rev.* **1990**, *5*, 13-29.
36. Sims, D.A.; Gamon, J.A. Relationships between leaf pigment content and spectral reflectance across a wide range of species, leaf structures and developmental stages. *Remote Sens. Environ.* **2002**, *81*, 337-354.
37. Netto, A.T.; Campostrini, E.; Oliveira, J.G.d.; Bressan-Smith, R.E. Photosynthetic pigments, nitrogen, chlorophyll a fluorescence and SPAD-502 readings in coffee leaves. *Sci. Hort.* **2005**, *104*, 199-209.

38. Wang, Y.Z.; Hong, W.; Wu, C.Z.; Lin, H.; Fan, H.L.; Chen, C.; Li, J. Variation of SPAD values in uneven-aged leaves of different dominant species in Castanopsis carlessi forest in Lingshishan National Forest Park. *J. For. Res.* **2009**, *20*, 362-366.
39. Markwell, J.; Osterman, J.C.; Mitchell, J.L. Calibration of the Minolta SPAD-502 leaf chlorophyll meter. *Photosynth. Res.* **1995**, *46*, 467-472.
40. Gratani, L. A nondestructive method to determine chlorophyll content of leaves. *Photosynthetica* **1992**, *26*, 469-473.
41. Monje, O.A.; Bugbee, B. Inherent limitations of nondestructive chlorophyll meters: A comparison of 2 types of meters. *Hortscience* **1992**, *27*, 69-71.
42. Marquard, R.D.; Tipton, J.L. Relationship between extractable chlorophyll and an insitu method to estimate leaf greenness. *Hortscience* **1987**, *22*, 1327-1327.
43. Schaper, H.; Chacko, E.K. Relation between extractable chlorophyll and portable chlorophyll meter readings in leaves of 8 tropical and subtropical fruit-tree species. *J. Plant Physiol.* **1991**, *138*, 674-677.
44. Castelli, F.; Contillo, R.; Miceli, F. Non-destructive determination of leaf chlorophyll content in four crop species. *J. Agron. Crop Sci.* **1996**, *177*, 275-283.
45. Yamamoto, A.; Nakamura, T.; Adu-Gyamfi, J.J.; Saigusa, M. Relationship between chlorophyll content in leaves of sorghum and pigeonpea determined by extraction method and by chlorophyll meter (SPAD-502). *J. Plant Nutrit.* **2002**, *25*, 2295-2301.
46. Uddling, J.; Gelang-Alfredsson, J.; Piikki, K.; Pleijel, H. Evaluating the relationship between leaf chlorophyll concentration and SPAD-502 chlorophyll meter readings. *Photosynth. Res.* **2007**, *91*, 37-46.
47. De Michele, C.; Vuolo, F.; D'Urso, G.; Marotta, L.; Richter, K. The Irrigation Advisory Program of Campania Region: From Research to Operational Support for the Water Directive in Agriculture. In *Proceedings of 33rd International Symposium on Remote Sensing of Environment*, Stresa, Italy, 4–8 May 2009; Volume II, pp. 965-968.
48. D'Urso, G.; Belmonte, C.A. Operative approaches to determine crop water requirements from earth observation data: Methodologies and applications. *AIP Conf. Proc.* **2006**, *852*, 14-25.
49. Leblanc, S.G.; Chen, J.M. A practical scheme for correcting multiple scattering effects on optical LAI measurements. *Agric. For. Meteorol.* **2001**, *110*, 125-139.
50. Migdall, S.; Bach, H.; Bobert, J.; Wehrhan, M.; Mauser, W. Inversion of a canopy reflectance model using hyperspectral imagery for monitoring wheat growth and estimating yield. *Prec. Agr.* **2009**, *10*, 508-524.
51. Chen, J.M.; Black, T.A. Defining leaf area index for non-flat leaves. *Plant Cell Environ.* **1992**, *15*, 421-429.
52. Neumann, H.H.; Den Hartog, G.; Shaw, R.H. Leaf area measurements based on hemispheric photographs and leaf-litter collection in a deciduous forest during autumn leaf-fall. *Agric. For. Meteorol.* **1989**, *45*, 325-345.
53. Darvishzadeh, R.; Skidmore, A.; Schlerf, M.; Atzberger, C. Inversion of a radiative transfer model for estimating vegetation LAI and chlorophyll in a heterogeneous grassland. *Remote Sens. Environ.* **2008**, *112*, 2592-2604.

54. Richter, K.; Hank, T.B.; Vuolo, F.; Mauser, W.; D'Urso, G. Optimal exploitation of the Sentinel-2 spectral capabilities for crop leaf area index mapping. *Remote Sens.* **2012**, *4*, 561-582.
55. Marchi, S.; Sebastiani, L.; Gucci, R.; Tognetti, R. Sink-source transition in peach leaves during shoot development. *J. Am. Soc. Hort. Sci.* **2005**, *130*, 928-935.
56. Haboudane, D.; Miller, J.R.; Tremblay, N.; Zarco-Tejada, P.J.; Dextraze, L. Heterogeneity of CASI-Estimated Chlorophyll Content: Assessment and Comparison with Ground Truth from L'ACADIE GEOIDE Experimental Site. Presented at *23rd Canadian Symposium on Remote Sensing*, Laval, QC, Canada, 20–24 August 2001.
57. Gandía, S.; Moreno, J.; Sagardoy, R.; Morales, F.; Verch, G. Crop Photosynthetic Pigment Composition and Calibration of an Instrument for Indirect Chlorophyll Content Determination. In *Proceedings of the Final Workshop for AGRISAR and EAGLE Campaigns*, Noordwijk, The Netherlands, 15–16 October 2007.
58. Richter, R. Correction of satellite imagery over mountainous terrain. *Appl. Opt.* **1998**, *37*, 4004-4015.
59. Bacour, C.; Baret, F.; Beal, D.; Weiss, M.; Pavageau, K. Neural network estimation of LAI, fAPAR, fcover and LAI×C<sub>(ab)</sub>, from top of canopy MERIS reflectance data: Principles and validation. *Remote Sens. Environ.* **2006**, *105*, 313-325.
60. Jacquemoud, S.; Verhoef, W.; Baret, F.; Bacour, C.; Zarco-Tejada, P.; Asner, G.; Francois, C.; Ustin, S. Prospect+SAIL models: A review of use for vegetation characterization. *Remote Sens. Environ.* **2009**, *113*, S56-S66.
61. Verhoef, W. Light-scattering by leaf layers with application to canopy reflectance modeling—The SAIL model. *Remote Sens. Environ.* **1984**, *16*, 125-141.
62. Myneni, R.B.; Hoffman, S.; Knyazikhin, Y.; Privette, J.L.; Glassy, J.; Tian, Y.; Wang, Y.; Song, X.; Zhang, Y.; Smith, G.R.; *et al.* Global products of vegetation leaf area and fraction absorbed par from year one of MODIS data. *Remote Sens. Environ.* **2002**, *83*, 214-231.
63. Shabanov, N.V.; Huang, D.; Yang, W.Z.; Tan, B.; Knyazikhin, Y.; Myneni, R.B.; Ahl, D.E.; Gower, S.T.; Huete, A.R.; Aragao, L.E.O.C.; *et al.* Analysis and optimization of the MODIS leaf area index algorithm retrievals over broadleaf forests. *IEEE Trans. Geosci. Remote Sens.* **2005**, *43*, 1855-1865.
64. Knyazikhin, Y.; Martonchik, J.V.; Myneni, R.B.; Diner, D.J.; Running, S.W. Synergistic algorithm for estimating vegetation canopy leaf area index and fraction of absorbed photosynthetically active radiation from MODIS and MISR data. *J. Geophys. Res.-Atmospheres* **1998**, *103*, 32257-32275.
65. Cohen, W.B.; Maersperger, T.K.; Gower, S.T.; Turner, D.P. An improved strategy for regression of biophysical variables and Landsat ETM+ data. *Remote Sens. Environ.* **2003**, *84*, 561-571.
66. Wang, Y.J.; Woodcock, C.E.; Buermann, W.; Stenberg, P.; Voipio, P.; Smolander, H.; Hame, T.; Tian, Y.H.; Hu, J.N.; Knyazikhin, Y.; *et al.* Evaluation of the MODIS LAI algorithm at a coniferous forest site in Finland. *Remote Sens. Environ.* **2004**, *91*, 114-127.
67. Huete, A.R. Soil and sun angle interactions on partial canopy spectra. *Int. J. Remote Sens.* **1987**, *8*, 1307-1317.

68. Bacour, C.; Jacquemoud, S.; Leroy, M.; Hautecoeur, O.; Weiss, M.; Prevot, L.; Bruguier, N.; Chauki, H. Reliability of the estimation of vegetation characteristics by inversion of three canopy reflectance models on airborne Polder data. *Agronomie* **2002**, *22*, 555-565.
69. Feret, J.B.; Francois, C.; Asner, G.P.; Gitelson, A.A.; Martin, R.E.; Bidel, L.P.R.; Ustin, S.L.; le Maire, G.; Jacquemoud, S. Prospect-4 and 5: Advances in the leaf optical properties model separating photosynthetic pigments. *Remote Sens. Environ.* **2008**, *112*, 3030-3043.
70. Kuusk, A. The Inversion of the Nilson-Kuusk Canopy Reflectance Model, A Test Case. In *Proceedings of IGARSS 91: Remote Sensing: Global Monitoring for Earth Management*, Espoo, Finland, 3–6 June 1991; Volume 1-4, pp. 1547-1550.
71. Kuusk, A. The Hot-Spot Effect in the Leaf Canopy. In *Proceedings of IGARSS 91: Remote Sensing: Global Monitoring for Earth Management*, Espoo, Finland, 3–6 June 1991; Volume 1–4, pp. 1555-1557.
72. Vuolo, F.; Atzberger, C.; Richter, K.; D'Urso, G.; Dash, J. Retrieval of Biophysical Vegetation Products from RapidEye Imagery. In *Proceedings of ISPRS TC VII Symposium "100 Years ISPRS"*, Vienna, Austria, 5–7 July 2010; pp. 281-286.
73. Huang, J.F.; Wang, F.M.; Wang, X.Z.; Tang, Y.L.; Wang, R.C. Relationship between narrow band normalized difference vegetation index and rice agronomic variables. *Commun. Soil Sci. Plant Anal.* **2004**, *35*, 2689-2708.
74. Gower, S.T.; Kucharik, C.J.; Norman, J.M. Direct and indirect estimation of leaf area index, fAPAR, and net primary production of terrestrial ecosystems. *Remote Sens. Environ.* **1999**, *70*, 29-51.
75. Chapman, S.C.; Barreto, H.J. Using a chlorophyll meter to estimate specific leaf nitrogen of tropical maize during vegetative growth. *Agron. J.* **1997**, *89*, 557-562.
76. Campbell, R.J.; Mobley, K.N.; Marini, R.P.; Pfeiffer, D.G. Growing conditions alter the relationship between SPAD-501 values and apple leaf chlorophyll. *Hortscience* **1990**, *25*, 330-331.
77. Sibley, J.L.; Eakes, D.J.; Gilliam, C.H.; Keever, G.J.; Dozier, W.A.; Himelrick, D.G. Foliar SPAD-502 meter values, nitrogen levels, and extractable chlorophyll for red maple selections. *Hortscience* **1996**, *31*, 468-470.
78. Gitelson, A.; Vina, A.; Ciganda, V.; Rundquist, D.; Arkebauer, T. Remote estimation of canopy chlorophyll content in crops. *Geophys. Res. Lett.* **2005**, *32*, 4.